

# Double-uncertainty optimal operation of hybrid AC/DC microgrids with high proportion of intermittent energy sources

Peng LI<sup>1</sup>, Pengfei HAN<sup>1</sup> , Shuai HE<sup>1</sup>, Xiaoxiao WANG<sup>1</sup>



**Abstract** This paper applies double-uncertainty optimization theory to the operation of AC/DC hybrid microgrids to deal with uncertainties caused by a high proportion of intermittent energy sources. A fuzzy stochastic expectation economic model for day-ahead scheduling based on uncertain optimization theory is proposed to minimize the operational costs of hybrid AC/DC microgrids. The fuzzy stochastic alternating direction multiplier method is proposed to solve the double-uncertainty optimization problem. A real-time intra-day unbalanced power adjustment model is established to minimize real-time adjustment costs. Through comparative analysis of deterministic optimization, stochastic optimization and fuzzy stochastic optimization of day-ahead scheduling and real-time adjustment, the validity of fuzzy stochastic optimization based on a fuzzy stochastic expectation model is proved.

**Keywords** Double-uncertainty optimization, Fuzzy stochastic ADMM, Fuzzy stochastic expected value model, High proportion of intermittent energy sources, Hybrid AC/DC microgrid

## 1 Introduction

Compared with the traditional power grid, microgrids have the potential advantages of high reliability and environmental friendliness, which can effectively compensate the shortcomings of centralized power generation and high voltage power transmission. Microgrids will be the main grid access for future loads and distributed generation, as an important part of smart distribution grids [1–6]. Microgrids can be divided into AC microgrids, DC microgrids and hybrid AC/DC microgrids [7]. Hybrid AC/DC microgrids are one of the most promising microgrid structures combining the advantages of AC and DC microgrids, which is convenient for integrating various forms of distributed generation and load [8, 9].

As the use of microgrids has increased rapidly, those with intermittent energy sources as the main energy supply have gradually become the most common kind. If the utility grid is used as an ideal power source to maintain a microgrid's internal real-time power balance, a high proportion of intermittent generation will cause too much disturbance to the utility grid, affecting its safety and stable operation. Necessarily, microgrids should develop an accurate day-ahead generation schedule and report it to the utility grid operator, and also minimize unbalanced power internally caused by intermittent energy output fluctuations. In hybrid AC/DC microgrids, due to their complicated internal structure, it is necessary to coordinate a mixture of AC and DC electrical equipment, which brings challenges to achieving optimized operation.

CrossCheck date: 26 September 2017

Received: 24 July 2017 / Accepted: 26 September 2017 / Published online: 20 November 2017

© The Author(s) 2017. This article is an open access publication

✉ Pengfei HAN  
ncepuhf@126.com

Peng LI  
ncepulp@ncepu.edu.cn

Shuai HE  
ncepuair@163.com

Xiaoxiao WANG  
ncepuxj@163.com

<sup>1</sup> Department of Electrical and Electronic Engineering, North China Electric Power University, Baoding 071003, Hebei Province, China

At present, research on hybrid AC/DC microgrids is mainly focused on their control strategy, whereas there is relatively little research on their optimal operation [10]. In [11], a multi-time-scale optimization model, which adjusts the power distribution by considering the impact of real-time electricity prices and unbalanced power, is proposed to maximize the revenue of hybrid AC/DC microgrids. However, the cost model does not take into account the energy storage charge and discharge costs due to round-trip losses. In [5] a two-layer optimization control model is proposed, which includes the system layer and the equipment layer. The system layer model optimizes the unit combination to realize the power balance, and the equipment layer is designed to stabilize the AC and DC voltages. However, neither paper discusses the negative effects of uncertainty from intermittent energy on the operation of hybrid AC/DC microgrids. The output power of widely used intermittent energy sources, such as wind power and photovoltaic power, often deviate from the predicted value.

This paper applies the double uncertainty optimization theory to the operation of hybrid AC/DC microgrids, to provide decision support to microgrid operators, and to enhance the ability of microgrids to cope with the uncertainty of power generation. It is assumed that microgrids are operated independently of the utility grid, though connected to it, based on a dispatch cycle and scheduling method similar to those used for the utility grid. Microgrid dispatch can be automated or, for large microgrids, supervised by a human operator.

Hybrid AC/DC microgrids are assumed to include wind turbines (WT), solar photovoltaic (PV) generators, energy storage (ES) and other distributed energy (DE) resources. A fuzzy stochastic optimization model for the operating cost and a real-time unbalanced power adjustment cost model are established, accounting for the characteristics of microgrid structure and the fluctuations of output power caused by intermittent generation. In response to the characteristics of the model, the alternating direction multiplier method (ADMM) is used to solve this problem. Finally, three models including deterministic optimal scheduling, optimal scheduling considering the randomness of intermittent generation, and optimal scheduling that considers double uncertainty are compared to verify the validity of the double-uncertainty optimization model and the algorithm.

## 2 Double-uncertainty optimal model

### 2.1 Overview of fuzzy stochastic optimization theory

In the theory of uncertainty, fuzziness and randomness are the two major uncertainties in complex decision-making, as shown in Fig. 1. Fuzziness reflects the lack of

sufficient information about the system, described by the fuzzy variable, while randomness is derived from the natural uncertainty in the system, characterized by stochastic variable. Since fuzziness and randomness exist simultaneously in complex decision-making, it is inadequate to consider only one or the other. Therefore, Kwakernaak [12] proposed fuzzy stochastic optimization theory to deal with such complex decision problems.

#### 2.1.1 Fuzzy stochastic variable

The essence of a fuzzy stochastic variable is a random variable with a fuzzy value, and it can be formally defined as follows. Consider a probability space  $(\Omega, A, Pr)$  with domain  $\Omega$  and probability  $Pr()$  that an element of  $\Omega$  is within the set  $A$ . Assuming that  $\xi$  is a function from the probability space  $(\Omega, A, Pr)$  to the fuzzy set, if for any Borel set  $B$  on real number field  $R$ , and any  $\omega$  in  $\Omega$ ,  $Pos\{\xi(\omega) \in B\}$  is a measurable function of  $\omega$ , then  $\xi$  is a fuzzy stochastic variable.

#### 2.1.2 Fuzzy stochastic optimization model

According to Fig. 1, fuzzy stochastic optimization models include the expected value model, the opportunistic constraint planning model and the related opportunistic constraint planning model [13]. The expected value model is widely used in power system optimization under uncertainty due to its intuitive appeal and simple solution, making it suitable for engineering optimization in a double-uncertainty environment [14, 15]. It is formulated as:

$$\begin{cases} \min E[f(\mathbf{x}, \xi)] \\ \text{s.t.} \\ E[g_j(\mathbf{x}, \xi)] \leq 0 \quad j = 1, 2, \dots, p \end{cases} \quad (1)$$

$$E[f(\mathbf{x}, \xi)] = \int f(\mathbf{x}, \xi)\phi(\xi)d\xi \quad (2)$$

where  $\mathbf{x}$  is the decision vector;  $\xi$  denotes fuzzy stochastic vector;  $E(\cdot)$  is the expected value operator;  $g_j$  denotes the  $j$ -th constraint.

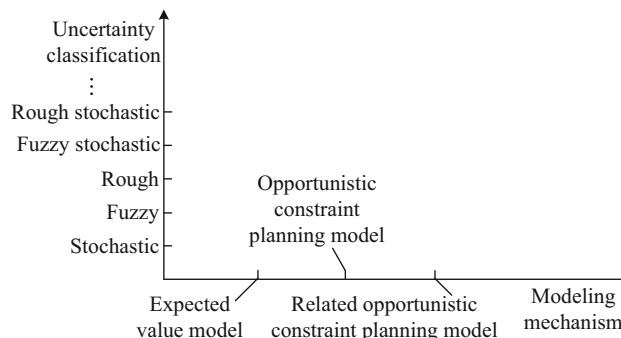


Fig. 1 Uncertainty classification and its modeling mechanism



Equation (1) gives the typical form of fuzzy stochastic planning expected value model. For the continuous fuzzy stochastic vector, as shown in (2), the expected value operator is the integral of the uncertain variable.

Compared with the utility grid, microgrids have the characteristics of relatively small scale and high levels of intermittent energy sources. If the microgrid operators ignore the uncertainty caused by the high proportion of intermittent energy, the scheduling of controllable microgrid resources will deviate greatly an optimal scheme. Stochastic optimization can adjust the prediction of intermittent energy output according to the probability distribution of uncertain variables. However, it is difficult to estimate the prediction deviation for stochastic optimization. Fuzzy stochastic variables can address this difficulty and can compensate for the shortcomings of stochastic variables in modeling typical probability distributions.

### 2.2 Fuzzy stochastic model of intermittent energy

In microgrid optimal scheduling, understanding the uncertainty of WT and PV output can be effective in reducing output prediction errors [16]. In the existing methods for optimal operation under uncertainty, the WT and PV outputs are treated as stochastic variables that follow specific probability distributions. It is still difficult to avoid obvious errors between the actual and predicted output, which leads to sub-optimal day-ahead scheduling. Since the prediction error does not follow a specific probability distribution, fuzzy set theory can be applied to analyze the prediction bias [17]. In this paper, PV and WT outputs in AC/DC hybrid microgrids are represented by fuzzy stochastic models. The predicted outputs are stochastic variables based on wind speed and light intensity predictions, and the error between the stochastic variables and the actual output is treated as a fuzzy variable. As shown in (3), the sum of the stochastic variable and the fuzzy variable is the fuzzy stochastic variable [13], where  $P_{\ell,random}$  and  $P_{\ell,fuzzy}$  represent the stochastic and fuzzy portions of the output power, respectively.

$$P_{\ell} = P_{\ell,random} + P_{\ell,fuzzy} \quad \ell \in \{PV, WT\} \tag{3}$$

Assuming that light intensity is a stochastic variable that obeys the  $\beta$  distribution, then (4) is the probability density function of PV output based on  $\beta$  distribution. Assuming that wind speed is a stochastic variable that obeys two-parameter Weibull distribution [18–20], then (5) is the probability density function of the wind speed based on two-parameter Weibull electrical. In these equations,  $\alpha$  and  $\beta$  denote the shape parameters of  $\beta$  distribution,  $P_{PV}(P_{PV,max})$  is the (maximum) output of the PV generator,  $v$  represents the wind speed,  $k$  and  $c$  are the shape parameter and scale parameter for two-parameter Weibull distribution,

respectively,  $c = \bar{v}/(1 + 1/k)$ , and  $\bar{v}$  is the average wind speed for the time period being modeled.

$$f(P_{PV}) = \frac{\Gamma(\alpha + \beta)}{P_{PV,max} \Gamma(\alpha) \Gamma(\beta)} \left( \frac{P_{PV}}{P_{PV,max}} \right)^{\alpha-1} \left( 1 - \frac{P_{PV}}{P_{PV,max}} \right)^{\beta-1} \tag{4}$$

$$f(v) = \frac{k}{c} \left( \frac{v}{c} \right)^{k-1} e^{-\left(\frac{v}{c}\right)^k} \tag{5}$$

The errors between the predicted and actual WT and PV outputs are treated as a fuzzy variables. The relative error calculated according to (6) is used in the fuzzy variable membership function [21] shown in (7):

$$\Delta\kappa = \frac{\kappa_{actual} - \kappa_{forecast}}{\kappa_{forecast}} \quad \kappa \in \{G, v\} \tag{6}$$

$$\mu_{\kappa} = \begin{cases} \left[ 1 + \eta_{\kappa} \left( \frac{\Delta\kappa}{\kappa^+} \right)^2 \right]^{-1} & \Delta\kappa \geq 0 \\ \left[ 1 + \eta_{\kappa} \left( \frac{\Delta\kappa}{\kappa^-} \right)^2 \right]^{-1} & \Delta\kappa < 0 \end{cases} \tag{7}$$

where  $G$  indicates the light intensity;  $\kappa^+$  is the average error percentage when the wind speed or light intensity is greater than the predicted value;  $\kappa^-$  is the average error percentage when it is less;  $\eta_{\kappa}$  is the weight factor.

Figure 2 is the membership function curve of the wind speed and light intensity relative prediction error.

### 2.3 Distributed generation operating cost model

#### 2.3.1 Energy storage operating cost model

Energy storage plays an important role in stabilizing the power fluctuations and reducing peak loads in a microgrid. With current technologies, battery energy storage capital costs are high, and energy storage costs account for a large proportion of capital costs of microgrids with large energy storage capacity [22]. Scheduling energy storage so that operating costs are reduced while ensuring the full benefit

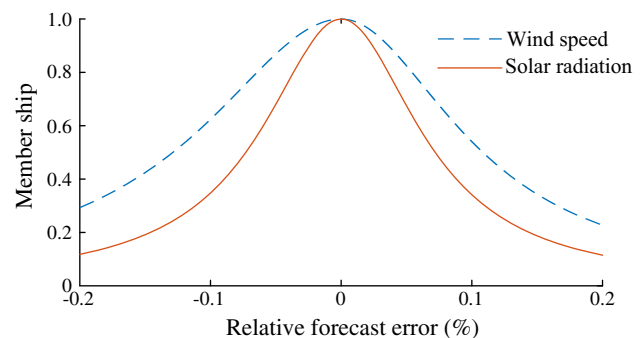


Fig. 2 Membership functions of wind speed and solar radiation forecast error

of energy storage is achieved, can effectively reduce the overall operating costs of microgrids.

The operating cost of energy storage include two main components: battery depreciation cost and energy loss during a charging and discharging cycle. The cost of energy storage depreciation has been estimated in [23]. The cost of energy lost during charging and discharging is estimated using the electricity price that is applicable in the microgrid, which will be a combination of the utility grid power price and the local price based on generation resources in the microgrid; the utility price is used in this paper. Using these, the integrated operating cost of energy storage  $C_{ES}(P)$  charging or discharging at a power  $P$  is given by (8).

$$C_{ES}(P) = P\Delta T \left[ I \frac{-vP\Delta T + 2Q(vSOC_{init} + l)}{2QA_{total} + (1 - \eta)^2 c_0'} \right] \quad (8)$$

where  $c_0'$  is the TOU (time of use) price of utility grid power during the  $t$ -th scheduled period;  $\Delta T$  is the scheduling time interval, taken as 15 min in this paper;  $\eta$  is the energy storage charge and discharge efficiency;  $Q$  is the storage capacity;  $l$  and  $v$  are the two empirical parameters to linearize effective electricity consumption [24], which are given values of 2.05 and  $-1.5$  respectively in this paper;  $A_{total}$  is the total discharge capacity that the battery can sustain during its effective life, which is assumed to be  $390Q$  in this paper;  $I$  is the initial investment in energy storage; and  $SOC_{init}$  is the initial state of charge.

### 2.3.2 Controllable distributed generation

In order to ensure stable operation in a variety of situations, controllable distributed generation is essential in microgrids alongside intermittent energy sources. Diesel generation is assumed in this paper and the fuel cost model is shown in (9), where  $C_{Fuel}$  is the cost of diesel fuel and  $P_{DE}^t$  is the output of the diesel generator during the  $t$ -th period.  $a_2$ ,  $a_1$  and  $a_0$  are polynomial coefficients of the consumption characteristic function of DE respectively, whose value are shown in Table A1 of Appendix A.

$$C_{Fuel} = \Delta T \sum_{t=1}^T (a_2 P_{DE}^2 + a_1 P_{DE}^t + a_0) \quad (9)$$

## 2.4 Fuzzy stochastic expectation optimization model for hybrid AC/DC microgrids

### 2.4.1 Objective function and constraints

The goal of an independent microgrid operator is to maximize operating profit while ensuring reliable microgrid operation. Reducing operating costs is the most

effective way to increase revenue when load and electricity price are relatively stable. The operating cost of grid-connected hybrid AC/DC microgrids includes the purchase cost of utility grid power, diesel (and other) fuel costs, transmission loss costs, energy storage costs and equipment maintenance costs.

A hybrid AC/DC microgrid consists of AC and DC zones, which are connected by one or more power flow controllers to achieve power balance. Comprehensive costs  $C_c$  are divided into the costs of the AC area  $C_{c,AC}$  and the costs of the DC area  $C_{c,DC}$ . The optimization model proposed in this paper is based on a typical hybrid AC/DC microgrid structure as shown in Fig. 3, where the AC side and the DC side both have loads and generators (including battery energy storage), and the utility grid connection is to the AC side. The cost components are summarized in (10).

$$\begin{cases} C_c = C_{c,AC} + C_{c,DC} \\ C_{c,AC} = C_{Grid} + C_{Fuel} + C_{ACloss} + C_{ACom} \\ C_{c,DC} = C_{ES} + C_{DCloss} + C_{DCom} \end{cases} \quad (10)$$

where  $C_{ES}$  is the operating cost of energy storage calculated by (8);  $C_{Fuel}$  is the cost of diesel fuel calculated by (9);  $C_{Grid}$  is the purchase cost for utility grid power, defined by (11).

$$C_{Grid} = \Delta T \sum_{t=1}^T (P_G^t c_0^t) \quad (11)$$

where  $c_0^t$  is the TOU price of utility grid power during the  $t$ -th scheduled period as used in (8);  $P_G^t$  is the power imported from the utility grid.

$C_{loss}$  is the cost of power transmission and conversion losses. As microgrids require only short transmission distances, the losses caused by line impedance are very small compared to total losses [25]. Therefore, only the losses caused by converters, transformers and power flow controllers are taken into account in this model. The transmission and conversion costs of the AC area can be expressed by (12).

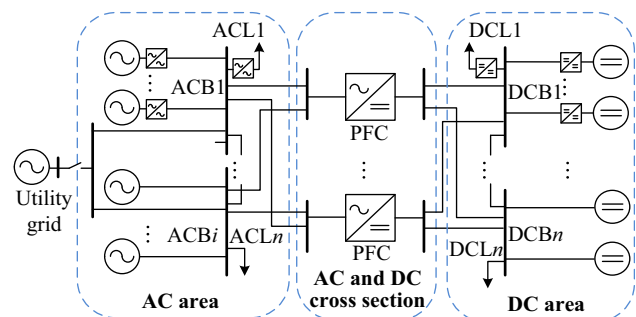


Fig. 3 Typical structure of hybrid AC/DC microgrid

$$\begin{aligned}
 C_{ACloss} = & \text{diag} \left[ \mathbf{P}_{DEV1,1}, \dots, \mathbf{P}_{DEV1,N_1}, \mathbf{P}_{DEV1,N_1+1}, \dots, \mathbf{P}_{DEV1,N_1+M_1} \right] \\
 & \times \text{diag} \left[ (1 - \eta_{1,1}), (1 - \eta_{1,2}), \dots, (1 - \eta_{1,N_1}), \underbrace{0, \dots, 0}_{M_1} \right] \\
 & \times \text{diag} \left[ \underbrace{c_0, \dots, c_0}_{N_1+M_1-H_1}, \underbrace{0, \dots, 0}_{H_1} \right] \times \Delta T
 \end{aligned} \tag{12}$$

where subscript 1 indicates the AC area;  $\mathbf{P}_{DEV1,i}$  represents the output power of the  $i$ -th power plant in the AC area during the modelling period;  $c_0$  is the TOU price vector for utility grid power during the modelling period;  $\mathbf{P}_{DEV1,i}$  and  $c_0$  are  $T$ -dimensional vectors. In the AC area there are  $N_1$  devices connected to the AC bus through transformers with efficiency  $\eta_{1,i}$ ;  $M_1$  devices are connected directly to the AC bus; there are  $H_1$  controllable devices and  $N_1 + M_1 - H_1$  uncontrollable devices in the AC area.

The cost of power transmission and conversion losses in the DC area can be expressed in a similar form. Losses in the power flow controllers can be included in either the AC or the DC area losses. If they are assigned to the DC area, the cost of DC area power transmission and conversion losses can be calculated using (13).

$$C_{DCloss} = \left\{ \begin{aligned} & \text{diag} \left[ \mathbf{P}_{DEV2,1}, \dots, \mathbf{P}_{DEV2,N_2}, \dots, \mathbf{P}_{DEV2,N_2+M_2} \right] \times \\ & \text{diag} \left[ (1 - \eta_{2,1}), (1 - \eta_{2,2}), \dots, (1 - \eta_{2,N_2}), \underbrace{0, \dots, 0}_{M_2} \right] \times \\ & \text{diag} \left[ \underbrace{c_0, \dots, c_0}_{N_2+M_2-H_2}, \underbrace{0, \dots, 0}_{H_2} \right] + \sum_{i=1}^{N_2+M_2} \left( \left| \mathbf{P}_{DEV2,i} \right| (1 - \eta_0) \times c_0^T \right) \end{aligned} \right\} \Delta T \tag{13}$$

where subscript 2 indicates the DC area;  $c_0^T$  is the transpose of the TOU price vector;  $\eta_0$  is the transmission efficiency of the power flow controller(s);  $M_2$  devices are connected directly to the DC bus; there are  $H_2$  controllable devices and  $N_2 + M_2 - H_2$  uncontrollable devices in the DC area.

$C_{om}$  is the cost of equipment operation and maintenance, calculated by (14), where  $K_i$  is the operation and maintenance cost of the  $i$ -th item of equipment.

$$C_{om} = \Delta T \sum_{t=1}^T \sum_{i=1}^{N+M} \left( K_i \mathbf{P}_{DEV,i} \right) \tag{14}$$

where  $N = N_1 + N_2$ ; there are  $N_2$  devices connected to the DC bus through DC/DC converters;  $M = M_1 + M_2$ .

A variety of equality and inequality constraints should be applied. For hybrid AC/DC microgrids it is necessary to

satisfy the internal power balance constraint (15) and the point of common coupling transmission capacity constraint (16). For energy storage, it is necessary to satisfy the charge and discharge power capacity constraint (17), the energy capacity constraint (18), and the conservation of energy constraint (19). For diesel generators, it is necessary to satisfy the minimum start or stop time constraint (20), the power constraint (21), and the ramping constraint (22).

$$P_{DE}^t + P_G^t + P_{WT}^t + P_{PV}^t = P_{ACL}^t + P_{ES}^t + P_{DCL}^t \tag{15}$$

$$|P_G^t| \leq P_{G,max} \tag{16}$$

$$|P_{ES}^t| \leq P_{ES,max}^t \tag{17}$$

$$SOC_{min} \leq SOC^t \leq SOC_{max} \tag{18}$$

$$SOC^{t+1} = SOC^t + (\mu_{ch}\eta_{ch} + \mu_{dis}/\eta_{dis})P_{ES}^t\Delta T/Q \tag{19}$$

$$\begin{cases} \tau_{DE}^{off} \geq \tau_{DE}^{off,min} \\ \tau_{DE}^{on} \geq \tau_{DE}^{on,min} \end{cases} \tag{20}$$

$$S(t)P_{DE,min} \leq P_{DE}^t \leq S(t)P_{DE,max} \tag{21}$$

$$\Delta TP_{DE,max}^L \leq P_{DE}^{t+1} - P_{DE}^t \leq \Delta TP_{DE,max}^U \tag{22}$$

where  $P_{ACL}^t$  and  $P_{DCL}^t$  represent AC and DC area load during the  $t$ -th period, respectively;  $P_{G,max}$  is the point of common coupling transmission capacity;  $SOC^t$  is the state of charge of energy storage;  $SOC_{min}$  and  $SOC_{max}$  are the lower and upper limits of the state of charge;  $\mu_{ch}$  is the energy storage charging state (1 means charging and 0 means discharging);  $\mu_{dis}$  is the discharging state (1 means discharging and 0 means charging), with  $\mu_{ch} + \mu_{dis} = 1$ ;  $\tau_{DE}^{off}$  and  $\tau_{DE}^{on}$  are the off and on time intervals;  $P_{DE,min}$  and  $P_{DE,max}$  are the lower and upper limits of diesel generator output power;  $S(t)$  and  $\Delta P_{DE,max}$  are the operating state and maximum ramping rate of the diesel generator, respectively.

#### 2.4.2 Fuzzy stochastic expectation optimization model of hybrid AC/DC microgrid

The goal is to minimize the expected value of total operating costs  $\min E(C_{c,AC} + C_{c,DC})$ . This is a fuzzy stochastic expectation optimization model because it includes constraints applied to fuzzy stochastic variables. Constraints on other variables can be expressed directly in deterministic form. Therefore, the optimization model proposed in this paper is given by (23).

$$\begin{aligned}
 & \min E(C_{c,AC} + C_{c,DC}) \\
 & \text{s.t.} \\
 & \begin{cases} E(P_{DE}^t + P_G^t + P_{WT}^t + P_{PV}^t = P_{ACL}^t + P_{ES}^t + P_{DCL}^t) \\ |P_G^t| \leq P_{G,max} \\ |P_{ES}^t| \leq P_{ES,max}^t \\ SOC_{min} \leq SOC^t \leq SOC_{max} \\ SOC^{t+1} = SOC^t + (\mu_{ch}\eta_{ch} + \mu_{dis}/\eta_{dis})P_{ES}^t\Delta T/Q \\ P_{DE,min} \leq P_{DE}^t \leq P_{DE,max} \\ \Delta TP_{DE,max}^L \leq P_{DE}^{t+1} - P_{DE}^t \leq \Delta TP_{DE,max}^U \\ \tau_{DE}^{off} \geq \tau_{DE}^{off,min} \\ \tau_{DE}^{on} \geq \tau_{DE}^{on,min} \end{cases} \quad (23)
 \end{aligned}$$

2.4.3 Unbalanced power real-time adjustment model

By establishing a real-time cost model for unbalanced power, an optimal adjustment scheme for eliminating unbalanced power can be derived. As shown in (24), the real-time adjustment model includes two parts as for the operating costs: AC area adjustment costs and DC area adjustment costs. Because the cost models for fuel, power transmission and conversion losses, and energy storage losses are non-linear, the cost model for unbalanced power would take too much time to calculate directly. Therefore, the nonlinear cost model is linearized at the day-ahead schedule operation points, as shown in (25), to reduce the calculation time. In this equation,  $P_{It}^t$  is the dispatched output of device  $It$  from the day-ahead fuzzy stochastic optimization model, and  $\Delta P_{It}^t$  is the adjustment required to achieve power balance. In order to penalize unbalanced power, the real-time electricity price of utility grid power purchased to correct unbalanced power is higher than the price applying to day-ahead scheduling. In this paper the real-time electricity price is assumed to be 1.5 times the day-ahead electricity. This approximates a future pricing regime that could be established to incentivize microgrids to balance as far as possible using their internal resources [26, 27].

$$\begin{cases} \Delta C_c = \Delta C_{c,AC} + \Delta C_{c,DC} \\ \Delta C_{c,AC} = \Delta C_{Grid} + \Delta C_{Fuel} + \Delta C_{ACloss} + \Delta C_{ACCom} \\ \Delta C_{c,DC} = \Delta C_{ES} + \Delta C_{DCloss} + \Delta C_{DCCom} \end{cases} \quad (24)$$

$$\begin{cases} \Delta C_I = \sum_{t=1}^T \left[ \left( \frac{dC_{It}}{dP_{It}^t} \right) \Delta P_{It}^t \right] \\ It = \{Fuel, ES, ACloss, DCloss\} \end{cases} \quad (25)$$

There are additional equality and inequality constraints for power balancing within a dispatch interval: the power

balance constraint (26) and the equipment capacity constraint (27) for the microgrid; and the state of charge constraint (28) and the charging and discharging power balance constraint (29) for energy storage. For adjusting the diesel generator the unit start and stop constraints do not apply, because it only changes its power within a dispatch interval when it is already on.

$$\begin{cases} P_{DE}^t + P_G^t + P_{WT}^t + P_{PV}^t = P_{ACL}^t + P_{ES}^t + P_{DCL}^t + \Delta P_{\Sigma}^t \\ \Delta P_{\Sigma}^t = \Delta P_{ACL}^t + \Delta P_{ES}^t + \Delta P_{DCL}^t - (\Delta P_{DE}^t + \Delta P_G^t + \Delta P_{WT}^t + \Delta P_{PV}^t) \end{cases} \quad (26)$$

$$P_{It}^{min} \leq P_{It}^t + \Delta P_{It}^t \leq P_{It}^{max} \quad (27)$$

$$SOC_{min}^{ES} \leq SOC_{ES}^t + \Delta SOC_{ES}^t \leq SOC_{max}^{ES} \quad (28)$$

$$\begin{aligned}
 SOC^{t+1} + \Delta SOC^{t+1} &= (\mu_{ch}\eta_{ch} + \mu_{dis}/\eta_{dis}) \\
 &\times (P_{ES}^t + \Delta P_{ES}^t)\Delta T/Q_{ES} + SOC^t + \Delta SOC^t \end{aligned} \quad (29)$$

3 Fuzzy stochastic ADMM

The development of smart grid is accompanied by two characteristics. Firstly, the amount of data collected and analyzed in the dispatching process is rapidly increasing, so the required scheduling model and algorithm are more complicated. Secondly, data collection and storage are more decentralized to cope with the large quantity. Compared with conventional microgrids, hybrid AC/DC microgrids with a high proportion of distributed generation have a complex structure, large uncertainty and consequently are difficult to schedule. In order to reduce the requirement for communication bandwidth to provide full data to a centralized scheduling solution, distributed computing is an effective method to reduce the computational complexity and improve the efficiency of the calculation process. It can decouple the AC area and DC area costs. Therefore, it is helpful to find a distributed algorithm suitable for the analysis of data required by the microgrid dispatching process.

3.1 Alternating direction multiplier method

The alternating direction multiplier method (ADMM) is a distributed solution method based on dual decomposition and Lagrange multipliers for large-scale optimization. It has significant advantages in dealing with high-dimensional variables and big data [28]. A typical model solved by the ADMM is shown in (30). According to Lagrange multiplier method, the Lagrange function of the optimization model (30) can be expressed by (31).



$$\begin{aligned} & \min [f(\mathbf{x}) + g(\mathbf{z})] \\ & \text{s.t. } \mathbf{Ax} + \mathbf{Bz} = \mathbf{c} \end{aligned} \tag{30}$$

$$\begin{aligned} L_\rho(\mathbf{x}, \mathbf{y}, \mathbf{z}) = & f(\mathbf{x}) + g(\mathbf{z}) + \mathbf{y}^T(\mathbf{Ax} + \mathbf{Bz} - \mathbf{c}) \\ & + (\rho/2)\|\mathbf{Ax} + \mathbf{Bz} - \mathbf{c}\|_2^2 \end{aligned} \tag{31}$$

where  $\mathbf{y}$  is the Lagrange multiplier;  $\rho > 0$  is the penalty factor.

Equations (32)–(34) describe the iterative processes of the ADMM, and when the convergence condition (35) is satisfied, iteration can be stopped. The solution precision  $\varepsilon$  is a small positive number.

$$\mathbf{x}^{k+1} := \arg \min_{\mathbf{x}} L_\rho(\mathbf{x}, \mathbf{z}^k, \mathbf{y}^k) \tag{32}$$

$$\mathbf{z}^{k+1} := \arg \min_{\mathbf{z}} L_\rho(\mathbf{x}^{k+1}, \mathbf{z}, \mathbf{y}^k) \tag{33}$$

$$\mathbf{y}^{k+1} := \mathbf{y}^k + \rho(\mathbf{Ax}^{k+1} + \mathbf{Bz}^{k+1} - \mathbf{c}) \tag{34}$$

$$|\mathbf{x}^{k+1} - \mathbf{x}^k| \leq \varepsilon \tag{35}$$

### 3.2 Fuzzy stochastic ADMM

In the fuzzy stochastic programming model, the ADMM can't be used directly because of the existence of uncertain variables. An optimization algorithm based on the fuzzy stochastic ADMM is proposed in this paper to solve the hybrid AC/DC microgrid scheduling problem.

The optimization model (23) developed in section 2 can be summarized by (36), where  $\mathbf{P}_{AC,d}$  and  $\mathbf{P}_{AC,fs}$  are the decision vector and fuzzy stochastic vector of the AC area, and  $\mathbf{P}_{DC,d}$  and  $\mathbf{P}_{DC,fs}$  are the decision vector and fuzzy stochastic vector of the DC area, respectively.

$$\begin{aligned} & \min [E(C_{c,AC}(\mathbf{P}_{AC,d}, \mathbf{P}_{AC,fs})) + E(C_{c,DC}(\mathbf{P}_{DC,d}, \mathbf{P}_{DC,fs}))] \\ & \text{s.t.} \\ & \begin{cases} E[\sum \mathbf{P}_{AC,d} + \sum \mathbf{P}_{AC,fs} + \sum \mathbf{P}_{DC,d} + \sum \mathbf{P}_{DC,fs}] = E[\sum \mathbf{P}_{load}] \\ E[\mathbf{g}_{AC}(\mathbf{P}_{AC,d}, \mathbf{P}_{AC,fs})] \leq \mathbf{0} \\ E[\mathbf{g}_{DC}(\mathbf{P}_{DC,d}, \mathbf{P}_{DC,fs})] \leq \mathbf{0} \end{cases} \end{aligned} \tag{36}$$

For a continuous fuzzy stochastic variable, the expected value is the integral of the uncertain variable. Assuming that the WT and PV generators run at their maximum power point, they are uncontrolled power supplies, and therefore, the total operating costs of the AC and DC areas does not directly include the uncertain variables of the WT and PV output, so the expected value of the objective function in (36) is the objective function itself. Thus, the objective function can be expressed as:

$$\max E(C_{c,AC} + C_{c,DC}) = \max (C_{c,AC} + C_{c,DC}) \tag{37}$$

For constraints with fuzzy stochastic variables, uncertain variables can be transformed into pure quantities by

integration of uncertain variables. However, the probability density functions of the PV and WT output power are obtained from the probability density functions of light intensity and wind velocity, so if they are directly integrated the problem will be very difficult to solve. Therefore, stochastic and fuzzy simulation techniques are employed to indirectly obtain the expected values of fuzzy stochastic variables in this paper.

For the fuzzy stochastic variable  $P_{fs}$ , the predicted deviation  $\Delta \hat{P}_f$  can be generated by the fuzzy simulation technique, and the predicted value  $\hat{P}_s$  can be generated by the stochastic simulation technique. Using (5) we can derive a large number of fuzzy stochastic samples  $\hat{P}_{fs}$ . Let  $M_s$  be the number of stochastic and fuzzy simulations, and then referring to (38) the fuzzy stochastic variable can be changed into a pure variable.

$$E(P_{fs}) = \lim_{M_s \rightarrow \infty} \frac{1}{M_s} \sum_{i=1}^{M_s} [\hat{P}_s(1 + \hat{P}_f)] \tag{38}$$

Drawing on the above analysis, the fuzzy stochastic ADMM can be summarized into three main steps:

- 1) Fuzzy and stochastic simulation. In this step, uncertain variables are generated according to the corresponding stochastic and fuzzy distributions. Each summation of a fuzzy stochastic variable over  $M_s$  simulations gives an intermediate variable  $e$ .
- 2) Eliminate uncertain variables. Due to the law of large numbers,  $e/M_s$  is the expected value of the uncertain variable that summed to  $e$ . The double-uncertainty optimization model can then be transformed into a deterministic model.
- 3) Conventional ADMM iteration. Without uncertain variables, the ADMM has a natural advantage in solving this kind of optimization model, because of the appropriate structure in (36).

The flow chart of fuzzy stochastic ADMM is shown in Fig. 4.

## 4 Simulation based on engineering data

### 4.1 Basic data

This paper relies on data from a demonstration project to verify the fuzzy stochastic expectation optimization model and algorithm. Light intensity, wind speed, and TOU power price are given in Table A2 and Table A3 of Appendix A. The microgrid is simplified reasonably for the purpose of this presentation. There are bus-voltage loads and non-bus-voltage loads in the AC and DC areas, and the load forecast data are shown in Fig. 5. There are two 350

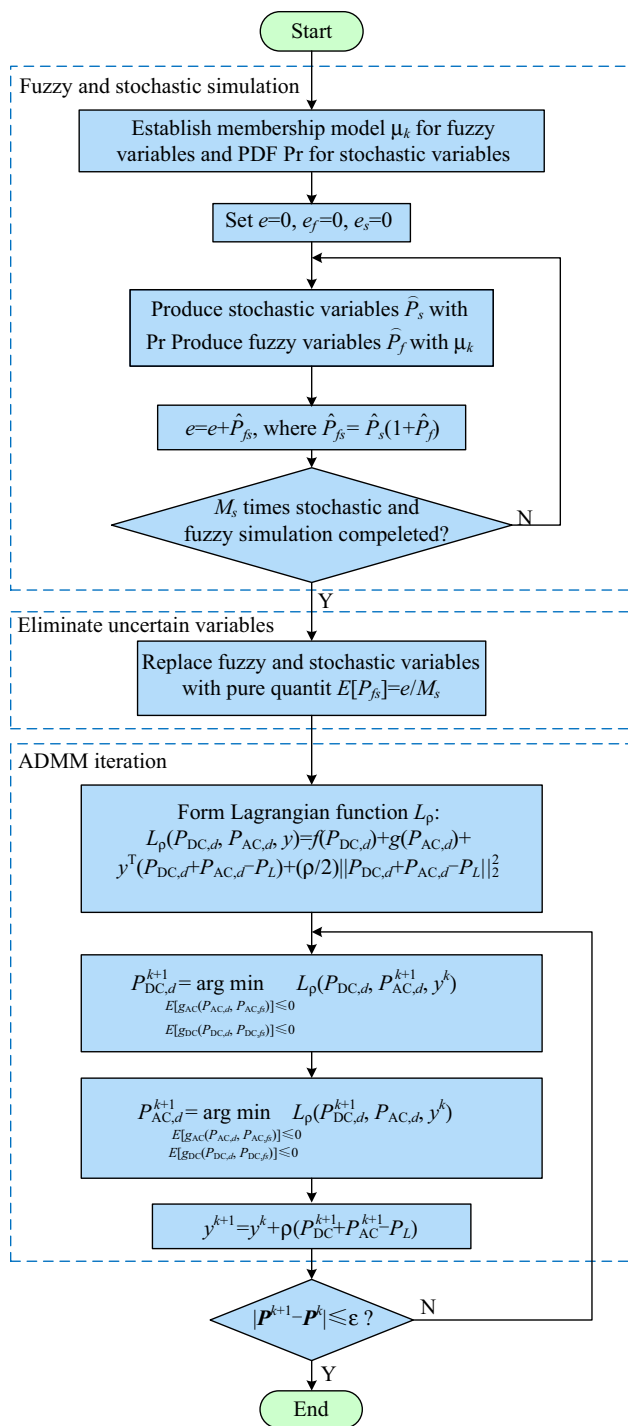


Fig. 4 Flow chart of fuzzy stochastic ADMM

kW diesel generators and two 1 MW WT in the AC area. The AC area is connected to the DC area through four 250 kW power flow controllers. The DC area contains four PV generation units each with capacity of 250 kW and one battery energy storage unit with power capacity 250 kW and energy capacity 1 MWh. The hourly predicted wind speed and light intensity data are shown in Fig. 6.

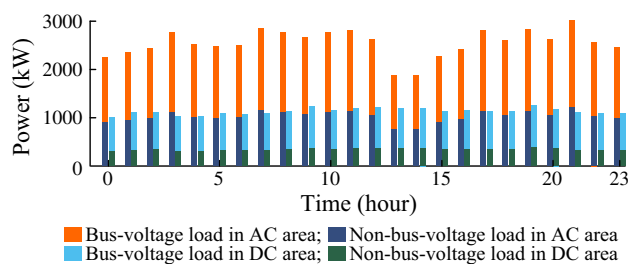


Fig. 5 Load forecast data in AC area and DC area

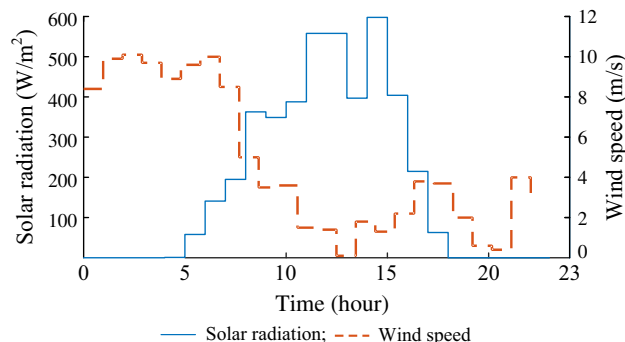


Fig. 6 Wind speed and solar radiation forecast data

Table 1 Parameters of distributed generators

Distributed generation	Min power (kW)	Max power (kW)	Number	Climbing rate (kW/h)	Operation costs (¥/kWh)
PV	0	250	4		0.0096
WT	0	1	2		0.0296
ES	-250	250	1		0.0880
DG	100	350	2	180	0.0755

Table 2 Power conversion equipment parameters

Converter equipment type	Efficiency ( $\beta$ is load rate)	Capacity (kW)	Number
Transformer	$\eta = \frac{1000\beta}{(6.44\beta^2 + 1000\beta + 47)}$	500	2
DC/DC converter	$\eta = -0.0215\beta^3 + 0.032\beta^2 - 0.0495\beta + 0.9844$	250	5
AC/DC PFC	$\eta = 0.2255\beta^3 - 0.4784\beta^2 + 0.3259\beta + 0.9084$	250	5

The operating parameters of the distributed generators are given in Table 1. In order to reduce the computational complexity, the loads with the same characteristics are combined without affecting the scheduling results. The amount of load-side power conversion equipment is reduced after the merger, and its efficiency, capacity and





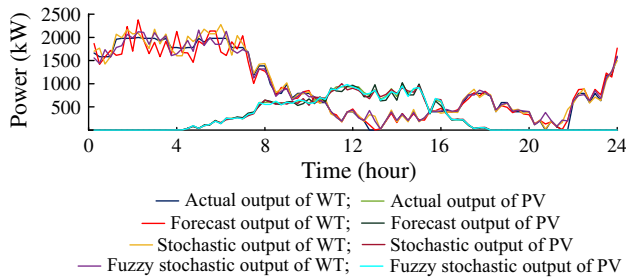


**Fig. 7** Deterministic, stochastic, fuzzy stochastic, and real outputs of WT and PV

quantity are given in Table 2, where the efficiency function is obtained by fitting measured data.

### 4.2 Simulation verification

In order to verify the advantages of the fuzzy stochastic optimization model relative to an existing optimization model, simulation results from fuzzy stochastic optimization are compared with deterministic optimization and stochastic optimization, the latter two being the most commonly used models at present. The deterministic and stochastic optimization models can be derived through appropriate simplification of the fuzzy stochastic optimization model.

The curves in Fig. 7 represent the actual (measured), deterministic, considering randomness and considering fuzzy randomness output of WT and PV generators. It can be seen that when different models of uncertainty are used, the corrections of WT and PV output are different. Using these four kinds of WT and PV output curves, the day-ahead schedule and unbalanced power adjustment are simulated for the load curves and microgrid components described above. The schedule comprises the power imported from the utility grid, the combination and output of the two diesel generators, and the charge and discharge power of the battery energy storage.

Figure 8 shows the deviation between the actual output and the output of the deterministic prediction, stochastic model, and fuzzy stochastic model. The error in estimating the WT and PV output is larger during 0:00~10:00, 12:00~13:00, and 21:00~24:00, because the renewable energy output in these times is larger and more sensitive to meteorological factors which are difficult to accurately predict. The deterministic error fluctuates greatly and reaches up to 400 kW more than once, while the absolute value of the deviation from stochastic expectation model is relatively small and the changes are more stable compared with the deterministic prediction; only at 22:00 does it reach up to 400 kW. The WT and PV output forecast by the fuzzy stochastic model is the closest to the actual output, with the smallest deviation, rarely more than 200 kW. The deviations

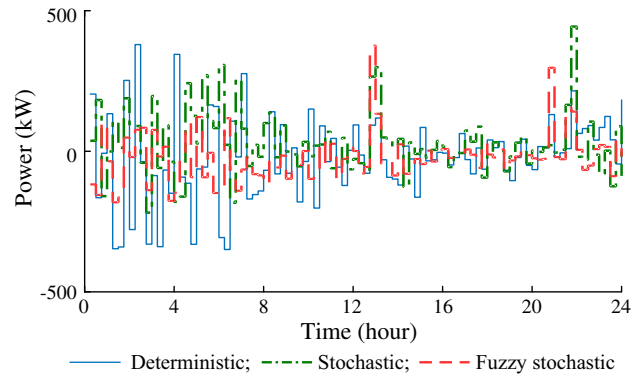


**Fig. 8** WT and PV outputs errors between deterministic, stochastic, and fuzzy stochastic optimization and the actual

graphed in Fig. 8 are the unbalanced power to be dispatched for real-time adjustment of the scheduled power.

Figures 9, 10 and 11 show the day-ahead schedule and real-time adjustment of controllable power in this hybrid

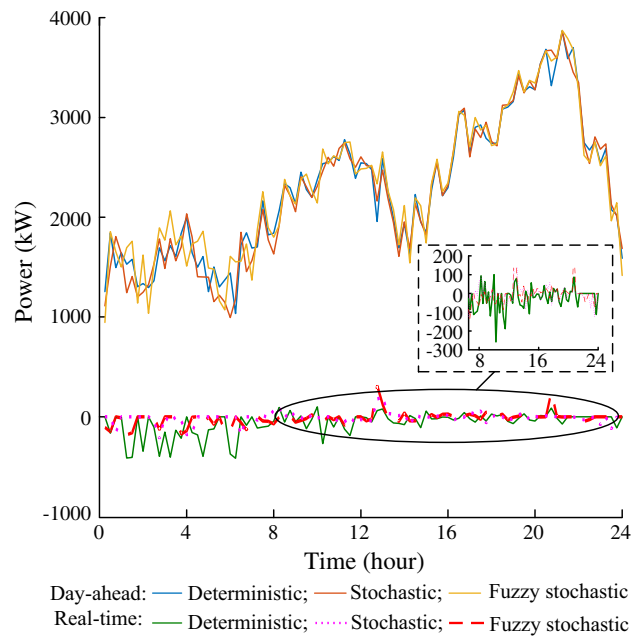


**Fig. 9** Output scheduling and real-time adjustment program of utility grid

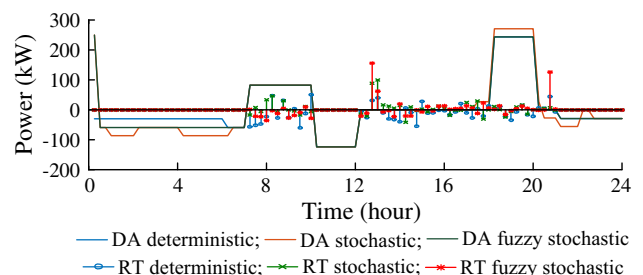


**Fig. 10** Energy storage planning and real-time adjustment

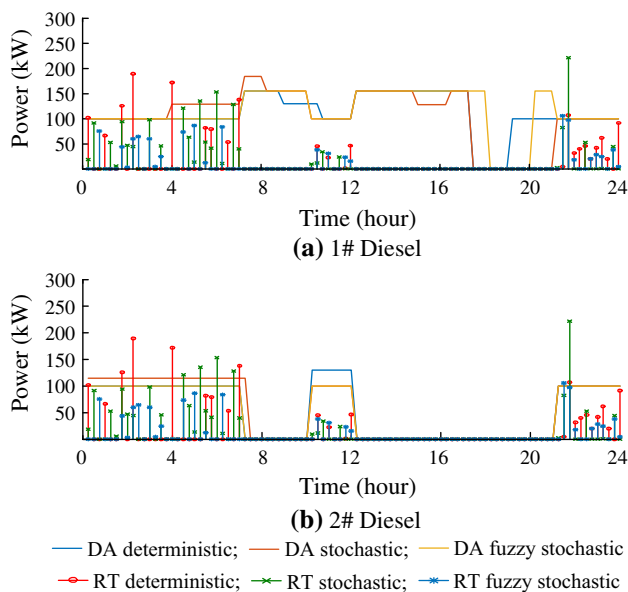


**Fig. 11** Diesel generator scheduling and real-time adjustment

AC/DC microgrid. It can be seen from Fig. 9 that, although the peak load of hybrid AC/DC microgrid and the installed capacity of renewable energy are equivalent, the capacity factors of WT and PV generation are relatively low, so the microgrid purchases power from the utility grid at all times. From the day-ahead schedule in Fig. 10, energy storage discharges when the electricity price is high, and charges when it is low, thereby reducing operating costs. In Fig. 11(a) and (b), the diesel power output is not sensitive to changing TOU power prices due to its output range and ramping constraints, but at least one diesel generator is consistently running during the period of high prices, to reduce the amount of utility power purchased. Due to the different fuel consumption characteristics of the two diesels, their output planning is different.

The unbalanced power adjustment schemes during each dispatch interval, for the four kinds of energy source, are obtained by the unbalanced power optimization model. It can be seen from the real-time adjustments shown in Figs. 8, 9 and 10 that the power needing to be adjusted is largest when using the deterministic optimization scheme, followed by the

**Table 3** Operating costs of each scheduling model

Type of schedule	Optimal (¥)	Deterministic (¥)	Stochastic (¥)	Fuzzy stochastic (¥)
Day-ahead schedule costs	46078	47831	45870	45939
Adjustment costs	0	- 158	559	290
Total costs	46078	47673	46429	46229

stochastic optimization model, and it is smallest when using the fuzzy stochastic optimization model. That is, the day-ahead scheme based on the fuzzy stochastic optimization model is the closest to the optimal scheme (the optimal schedule refers to the scheme obtained by optimizing according to the actual output instead of the prediction). It can also be seen that, during the energy storage discharge period (8:00 ~ 10:00, 12:00 ~ 18:00), the unbalanced power is mainly adjusted using energy storage and imported power from the utility grid. This is because the running diesel is close to its lower limit of operation during these times, and the flexibility and economy of the energy storage and power grid is better in this circumstance.

Table 3 summarizes the operating costs associated with the day-ahead schedule and unbalanced power adjustment for different scheduling models. The optimal scheme in the table is not a practical solution but is useful for comparing costs with the other three optimization models. We can see that although the stochastic optimization cost is less than the fuzzy stochastic model in the day-ahead scheduling stage, the daily adjustment cost of the stochastic model is higher than that of the fuzzy stochastic model. The total operating costs of the three optimization models, deterministic optimization, stochastic optimization and fuzzy stochastic optimization, are progressively reduced. In the unbalanced power adjustment, the deterministic model adjustment costs are negative, because the actual outputs of WT and PV are larger than the forecast values, the unbalanced power adjustment has reduced the amount of utility grid power purchased. The final operating cost of the fuzzy stochastic optimization scheme is only ¥151 more than the optimal operating cost.

Figure 12 shows the proportion of the various components of the total operating cost based on the fuzzy stochastic optimization model. It can be seen that the cost of purchasing utility grid accounts for the majority of the total cost of operation. In order from greatest to least, the other operating costs are the diesel operating costs, cost of power conversion losses, operation and maintenance costs and energy storage operating costs.

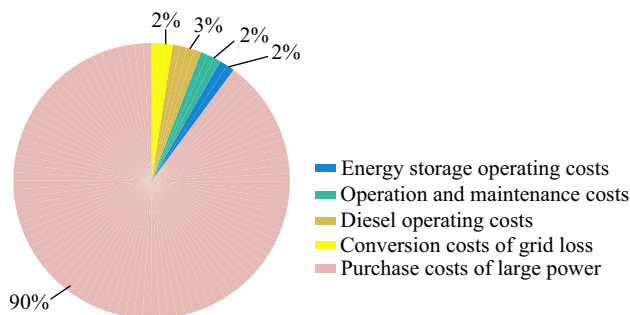


**Fig. 12** Fuzzy stochastic optimization of the operation of the cost ratio

## 5 Conclusion

Compared with deterministic optimization and stochastic optimization, the fuzzy stochastic expectation optimal scheduling model and the unbalanced power real-time adjustment model proposed in this paper can effectively improve the accuracy of microgrid scheduling when there is a high proportion of intermittent energy. The proposed models reduce the real-time unbalanced power, and thus reduce the costs of the unbalanced power adjustment. By cooperating with the fuzzy stochastic ADMM also proposed in this paper, the models can effectively coordinate various generators and loads in the AC and DC areas of a hybrid AC/DC microgrid, resulting in reduced total operating costs.

The prediction error of the load is also an uncertain factor in microgrid operation, so double-uncertainty optimal operation considering the load forecasting error, as well as the intermittent generation output forecasting error, is recommended as a topic for further study.

**Acknowledgements** This work was supported by the National Natural Science Foundation of China (No. 51577068) and Science & Technology Foundation of SGCC (No. 520201150012).

**Open Access** This article is distributed under the terms of the Creative Commons Attribution 4.0 International License (<http://creativecommons.org/licenses/by/4.0/>), which permits unrestricted use, distribution, and reproduction in any medium, provided you give appropriate credit to the original author(s) and the source, provide a link to the Creative Commons license, and indicate if changes were made.

## Appendix A

**Table A1** Diesel generator consumption characteristic coefficients

Diesel	$a_0$	$a_1$	$a_2$
1#	0.196	0.1465	0.0071
2#	0.184	0.1665	0.0061

**Table A2** Solar radiation and wind speed forecast

Time (h)	Solar radiation ( $W/m^2$ )	Wind speed (m/s)	Time (h)	Solar radiation ( $W/m^2$ )	Wind speed (m/s)
1	0	8.4	13	558	1.4
2	0	9.9	14	397	0.1
3	0	10.1	15	598	1.8
4	0	9.7	16	404	1.3
5	1	8.9	17	215	2.2

**Table A2** continued

Time (h)	Solar radiation ( $W/m^2$ )	Wind speed (m/s)	Time (h)	Solar radiation ( $W/m^2$ )	Wind speed (m/s)
6	58	9.6	18	63	3.8
7	141	10.0	19	0	3.7
8	195	8.5	20	0	2.0
9	363	5.0	21	0	0.6
10	349	3.5	22	0	0.4
11	388	3.6	23	0	4.0
12	558	1.5	24	0	3.2

**Table A3** TOU power price of the utility grid

Time (h)	Price (¥/kWh)	Time (h)	Price (¥/kWh)
1	0.457	13	0.941
2	0.457	14	0.941
3	0.457	15	0.941
4	0.457	16	0.941
5	0.457	17	0.941
6	0.457	18	0.941
7	0.457	19	1.123
8	0.941	20	1.123
9	0.941	21	0.941
10	0.941	22	0.457
11	0.457	23	0.457
12	0.457	24	0.457

Note: The price of microgrid power exported to the utility grid is assumed to be 0.43 ¥/kWh regardless of peak or valley periods

## References

- [1] Wang H, Huang J (2017) Incentivizing energy trading for interconnected microgrids. *IEEE Trans Smart Grid*. <https://doi.org/10.1109/TSG.2016.2614988>
- [2] Nguyen H, Khodaei A, Han Z (2016) A big data scale algorithm for optimal scheduling of integrated microgrids. *IEEE Trans Smart Grid*. <https://doi.org/10.1109/TSG.2016.2550422>
- [3] Zhao H, Wu QW, Wang C et al (2015) Fuzzy logic based coordinated control of battery energy storage system and dispatchable distributed generation for microgrid. *J Mod Power Syst Clean Energy* 3(3):422–428. <https://doi.org/10.1007/s40565-015-0119-x>
- [4] Li P, Gao J, Xu D et al (2016) Hilbert–Huang transform with adaptive waveform matching extension and its application in power quality disturbance detection for microgrid. *J Mod Power Syst Clean Energy* 4(1):19–27. <https://doi.org/10.1007/s40565-016-0188-5>
- [5] Baboli PT, Shahparasti M, Moghaddam MP et al (2014) Energy management and operation modelling of hybrid AC–DC microgrid. *IET Gener Transm Dis* 8(10):1700–1711
- [6] Liu Z, Hoidalén HK, Saha MM (2016) An intelligent coordinated protection and control strategy for distribution network

- with wind generation integration. *CSEE J Power Energy Syst* 2(4):23–30
- [7] Ma T, Cintuglu MH, Mohammed O (2015) Control of hybrid AC/DC microgrid involving energy storage, renewable energy and pulsed loads. In: *IEEE industry applications society annual meeting*, Addison, 18–22 October 2015, pp 1–8
- [8] Ding G, Gao F, Zhang S et al (2014) Control of hybrid AC/DC microgrid under islanding operational conditions. *J Mod Power Syst Clean Energy* 2(3):223–232. <https://doi.org/10.1007/s40565-014-0065-z>
- [9] Loh PC, Li D, Chai YK et al (2013) Autonomous operation of hybrid microgrid with AC and DC subgrids. *IEEE Trans Power Electr* 28(5):2214–2223
- [10] Nejabatkhah F, Li YW (2015) Overview of power management strategies of hybrid AC/DC microgrid. *IEEE Trans Power Electr* 30(12):7072–7089
- [11] Li P, Hua H, Di K et al (2016) Optimal operation of AC/DC hybrid microgrid under spot price mechanism. In: *IEEE power and energy society general meeting (PESGM)*, Boston, Massachusetts, 17–21 July 2016, pp 1–5
- [12] Hetzer J, David CY, Bhattacharai K (2008) An economic dispatch model incorporating wind power. *IEEE Trans Energy Convers* 23(2):603–611
- [13] Liu BD, Zhao RQ, Wang G (2003) *Uncertain programming with applications*. Press of Tsinghua University, Beijing, p 214
- [14] Ejaj AA, Shaaban MF, Ponnambalam K et al (2016) Stochastic centralized dispatch scheme for AC/DC hybrid smart distribution systems. *IEEE Trans Sustain Energy* 7(3):1046–1059
- [15] Jia L, Tong L (2016) Renewables and storage in distribution systems: centralized vs decentralized integration. *IEEE J Sel Area Commun* 34(3):665–674
- [16] Xiang Y, Liu J, Liu Y (2016) Robust energy management of microgrid with uncertain renewable generation and load. *IEEE Trans Smart Grid* 7(2):1034–1043
- [17] Valencia F, Sáez D, Collado J et al (2016) Robust energy management system based on interval fuzzy models. *IEEE Trans Control Syst Technol* 24(1):140–157
- [18] Aalami HA, Nojavan S (2016) Energy storage system and demand response program effects on stochastic energy procurement of large consumers considering renewable generation. *IET Gener Transm Dis* 10(1):107–114
- [19] Karki R, Hu P, Billinton R (2016) A simplified wind power generation model for reliability evaluation. *IEEE Trans Energy Convers* 21(2):533–540
- [20] Liang H, Tamang AK, Zhuang W et al (2014) Stochastic information management in smart grid. *IEEE Commun Surv Tut* 16(3):1746–1770
- [21] Liang RH, Liao JH (2007) A fuzzy-optimization approach for generation scheduling with wind and solar energy systems. *IEEE Trans Power Syst* 22(4):1665–1674
- [22] Zhao B, Wang CS, Zhang XS (2013) A survey of suitable energy storage for island stand-alone microgrid and commercial operation mode. *Autom Electric Power Syst* 37(4):21–27
- [23] Wang C, Liu N (2016) Distributed optimal dispatching of interconnected microgrid system based on alternating direction method of multipliers. *Proc CSEE* 40(9):2675–2681
- [24] Zhao B, Zhang X, Chen J et al (2013) Operation optimization of standalone microgrids considering lifetime characteristics of battery energy storage system. *IEEE Trans Sustain Energy* 4(4):934–943
- [25] Kakigano H, Miura Y, Ise T et al (2013) Basic sensitivity analysis of conversion losses in a dc microgrid. In: *2012 international conference on renewable energy research and applications (ICRERA)*, Nagasaki, Kyushu, Japan, 11–14 November 2012, pp 1–6
- [26] Parvania M, Khatami R (2017) Continuous-time marginal pricing of electricity. *IEEE Trans Power Syst* 32(3):1960–1969
- [27] Namerikawa T, Okubo N, Sato R et al (2015) Real-time pricing mechanism for electricity market with built-in incentive for participation. *IEEE Trans Smart Grid* 6(6):2714–2724
- [28] Boyd S, Parikh N, Chu E et al (2011) Distributed optimization and statistical learning via the alternating direction method of multipliers. *Found Trends Mach Learn* 3(1):1–122

**Peng LI** received the B.S., M.S. and Ph.D. degrees from the North China Electric Power University, China, in 1988, 1993 and 2004, respectively, all in electrical engineering. He is now a Full Professor with the North China Electric Power University, Baoding, China. His research interests include distributed generation, Microgrid, power quality analysis and control, power electronics technology application in power system, etc. He is a Senior Member of the IEEE.

**Pengfei HAN** received the B.S. degree from the North China Electric Power University, China, in 2015. He is currently a postgraduate from North China Electric Power University. His main research interests include distributed generation and microgrid technologies.

**Shuai HE** is currently pursuing the post-graduate degree in electrical engineering at North China Electric Power University. His current research interests include distributed generation and microgrid technology.

**Xiaoxiao WANG** is currently a postgraduate from North China Electric Power University. Her current research interests include distributed generation and microgrid technology.

